PROCEEDINGS OF SPIE

SPIEDigitalLibrary.org/conference-proceedings-of-spie

Superparamagnetic nanoparticles for the treatment of periodontal disease

Shayden Fritz, Leisha Armijo, Kayla Simpson, Kimberly Lopez, Marek Osinski, et al.

Shayden R. Fritz, Leisha M. Armijo, Kayla Simpson, Kimberly Lopez, Marek Osinski, Nihal Bandara, Hugh D. C. Smyth, Jian Sheng, Wei Xu, "Superparamagnetic nanoparticles for the treatment of periodontal disease," Proc. SPIE 12395, Colloidal Nanoparticles for Biomedical Applications XVIII, 1239509 (17 March 2023); doi: 10.1117/12.2654656



Event: SPIE BiOS, 2023, San Francisco, California, United States

Superparamagnetic nanoparticles for the treatment of periodontal disease

Shayden R. Fritz, Ab Leisha M. Armijo, Kayla Simpson, Kimberly Lopez, Marek Osinski, Nihal Bandara, Hugh D.C. Smyth, Jian Sheng and Wei Xu*a

aDepartment of Life Sciences, Texas A&M University-Corpus Christi, 6300 Ocean Drive, Corpus Christi, TX 78412, USA; Department of Physical and Environmental Sciences, Texas A&M University-Corpus Christi, 6300 Ocean Drive, Corpus Christi, TX 78412, USA; Department of Engineering, Texas A&M University-Corpus Christi, 6300 Ocean Drive, Corpus Christi, TX 78412, USA; USA; USA; USA; USA; USA; Department of Physical Albuquerque, NM 87106, USA; Bristol Dental School, University of Bristol, Lower Maudlin Street Bristol BS1 2YL, United Kingdom; Division of Molecular Pharmaceutics and Drug Delivery, College of Pharmacy, The University of Texas at Austin, 2409 University Ave, Austin TX, 78712,

ABSTRACT

USA

Periodontal diseases are prevalent worldwide and are linked to numerous other health conditions due to dysbiosis and chronic inflammatory state. Most periodontal diseases are caused by pathogenic bacteria that colonize dental tissues in the form of biofilm. Eradication of bacterial biofilms can be difficult to achieve due to the complex architecture of the teeth and gums which complicates the removal. Orthodontic wires and dental devices introduce additional hurdles to the adequate removal of biofilms by traditional methods since mechanical disruption via direct contact with toothbrush bristles, floss, and abrasive toothpaste is limited. Magnetically activated nanoparticles (NPs), specifically iron oxide nanoparticles (IONPs) that can be functionalized as antimicrobial particles and remotely controlled by magnetic fields, are of interest for oral biofilm eradication. We present data in multi-species bacterial cultures, established biofilms, human gingival keratinocytes, and human gingival fibroblast cells alone and in the presence of multispecies biofilm co-cultures to determine the safest, most efficacious IONP size ranges and treatment concentrations of active magnetic NPs for removal of dental biofilms. We report enhanced efficacy for IONPs coated with alginate vs. dextran, and small sizes (~8 nm vs. >20 nm in size) appear to exhibit enhanced antimicrobial efficacy. Human gingival keratinocyte (TIGK) cells in co-culture with treated and untreated multispecies biofilms in an *in-vitro* periodontitis model also exhibited a trend of reduced inflammatory markers in wells with IONP-treated biofilms.

Keywords: Iron oxide nanoparticles, periodontal disease, oral biofilms, *in vitro* co-culture, magnetic nanoparticles, antimicrobial drug

1. INTRODUCTION

Microorganisms are commonly found in nature, living in a biofilm state as aggregates that form a complex structure on different surfaces [1]. The bacteria in biofilms are protected against disinfection solution due to the scaffolds of biofilms due to the composition of the extracellular polymeric matric and DNA of microbial origins [2,3]. Over time, many bacteria have developed resistance to commonly used antibiotics, leading scientific and medical professionals to struggle with the intensifying antibiotic resistance problem [1,4]. Dental bacteria have microbial diversity and display high homeostatic capacity, which allows the bacteria to adapt to the changing oral environment and exposure to stresses metabolically [5]. The interaction between the dental bacterial species in the biofilm enables the growth, survival, and finding of their metabolic role within their polymicrobial community [5]. Oral bacteria have developed resistance to commonly used antibiotics and formulated dental care products and biofilm formation results in additional complications to sufficient oral hygiene. An efficient, easy-to-use antibiofilm agent to treat oral cavity infections is of interest.

Oral infections can range from mild gum diseases to severe periodontitis, which can result in pain and disability for millions of Americans and costs taxpayers billions of dollars each year [6]. Tooth decay is reported by 60% to 90% of

Colloidal Nanoparticles for Biomedical Applications XVIII, edited by Marek Osiński, Antonios G. Kanaras Proc. of SPIE Vol. 12395, 1239509 · © 2023 SPIE · 1605-7422 · doi: 10.1117/12.2654656

children and 100% of adults worldwide [7]. Dental biofilm persistence leads to a recurrent cycle of infection and inflammation that may contribute to various significant health problems. The currently available treatments are insufficient while requiring the consumer to follow a strict application schedule to which compliance is low. Triclosan has been used as an antibacterial drug and was found commonly in toothpaste, soaps, and other cosmetics. It was banned by the FDA in 2018 but is still found in some toothpaste. Chlorhexidine was found to be an effective compound against plaque and gingivitis; however this must be weighed against the potential risk for anaphylactic reactions [8]. Additionally, the efficacy of chlorhexidine for the prevention of cavities and periodontitis management does not appear to be well supported by the literature [8].

Nanoscale particles, as opposed to water-soluble molecular compounds, may be better equipped to penetrate the biofilm pores. The iron oxide nanoparticles (IONPs) investigated here are biofunctionalized to allow better penetration into the biofilm matrix. The positive charge of the iron is shielded by a negatively charged natural polymer to avoid sticking on the surface. The application of an external magnetic field (MF) to an infected area enhances the biofilm disruption action of IONPs. We previously reported on the antimicrobial effects of IONPs and enhanced effects with external magnetic field application [4, 9, 10]. Herein we present a snapshot of a work-in-progress in which we aim to optimize this system for use as a dental antimicrobial by investigating IONPs of different sizes, comparing Fe_2O_3 (red iron oxide) to Fe_3O_4 (black iron oxide), and comparing dextran with alginate as coating materials.

2. MATERIALS AND METHODS

2.1 Materials

Iron (III) chloride, oleic acid (90%), oleylamine, alginic acid sodium salt (low viscosity), dextran (Mr ~40 000), Fe(acac)₃, and phenyl ether were purchased from Sigma-Aldrich (St. Louis, MO, USA). Hexane, ethanol, and acetone were purchased from Fisher Chemical (Hanover Park, IL). Sodium oleate and 1,2-hexadecanediol were purchased from TCI America (Portland, OR). Fe₂O₃ (sample #3) and Fe₃O₄ (sample #4) NPs were purchased from SkySpring Nanomaterials (Houston, TX). All chemicals were used as received without further purification. The magnet used in these studies was a 2"×1"× 0.5" NdFeB grade 52 Ni-Cu-Ni coated magnet with a surface field of 4174 Gauss and Br_{max} of 14,800 Gauss and BH_{max} of 52 MGOe and was purchased from K&J Magnetics (Pipersville, PA).

2.2 Synthesis of IONPs

2.2.1. Method for synthesizing large IONPs (sample #1). IONPs were synthesized at a modified low-cost and high-yield green-chemistry solvothermal/solid-gas phase procedure [11]. Our specific modifications are described in [12]. In a typical procedure, iron (III) chloride (0.04 mol) was added to 25 mL of deionized (DI) water and stirred until completely dissolved. The solution was filtered with a filtering flask, plastic filter, filter paper, and vacuum hose; then slowly poured through the filter. The filtered mixture was added to a 500 mL reaction flask. Sodium oleate (36.5 grams) was then added into the reaction flask, opened to air, and gently stirred. 80 mL of ethanol and 140 mL of hexane were then added to the reaction vessel. The flask was then attached to a condenser and gas adapter with open necks sealed using a rubber septum and headed to 70 °C. The mixture was left for 24 hours under argon flow. After that, the solution was cooled to 50 °C, and the argon was turned off. Then the mixture was washed with deionized water in a separatory funnel three times. The hexane was then removed using a Rotovap set at 50-60 °C. The iron oleate complex (0.4 mol) was mixed with oleic acid (0.02 mol) in a reaction flask. 1-octadecene (0.792 mol) was added to the reaction flask. A large condenser was attached to the reaction flask, and the open neck was capped with a rubber septum. Argon flow was connected to the gas adapter on the condenser via the Schlenk line, and the solution was heated to 60 °C and stirred vigorously to allow the solvent to melt. The heat was then adjusted to 320 °C at a heating rate of ~3 °C per minute. The solution was refluxed for 30 minutes and then cooled to 50 °C. The completed IONPs were mixed with ethanol and centrifuged to precipitate and wash the particles. The washed IONPs were then stored in a hydrophobic solvent to prevent oxidation.

2.2.2 Method for synthesizing ultrasmall IONPs (sample #4). The ultrasmall iron oxide nanoparticles process was based on the methods from Sun, et al [13]. In a typical procedure, 20 mL phenyl ether is combined with 10 mmol of 1,2-hexadecanediol, 6 mmol oleic acid, 2 mmol of Fe(acac)₃, and 6 mmol oleylamine in a reaction flask, under stirring with a condenser, gas adapter, placed under nitrogen flow and refluxed for 30 minutes. The solution was cooled to room temperature, and then precipitated from the solution and washed with ethanol.

2.3 Functionalization of the IONPS

The four IONP samples of interest were separated evenly into two groups and functionalized with either dextran or alginate for surface coatings. The IONPs samples included sample #1 (described in 2.1.1), sample #2 (commercial Fe₂O₃ IONPs), sample #3 (commercial Fe₃O₄ IONPs), and sample #4 (described in 2.1.2).

- 2.3.1 IONP functionalization with dextran.5 grams of dextran was mixed in 100 mL milliQ water until dissolved. The dextran solution was mixed with 0.5 grams of the IONPs. The solution was stirred at 100 °C for 24 hours. The solution was then cooled to room temperature and centrifuged for 15 minutes at 800 rpm for separation.
- 2.3.2 IONP functionalization with alginate. A solution of 0.2 g IONPs per 20 mL of milliQ water was combined with alginate solution with a concentration of one gram per liter and stirred at 40 °C for 24 hours. The suspension was then centrifuged for 180 minutes at 3000 rpm to separate the coated particles from the supernatant.

2.4 Characterization of IONPs

- 2.4.1 Transmission Electron Microscopy (TEM). TEM was images were captured using the JEOL 1200 EX TEM operating at 100 kV using a tungsten filament and bottom mounted 3k x 3k slowscan lens-coupled CCD camera (SIA 15C).
- 2.4.2~X-ray Diffraction (XRD). The synthesized IONPs were placed in the sample holder of two circle goniometers, enclosed in a radiation safety enclosure. The X-ray source was a 1 kW Cu X-ray tube maintained at an operating current of 40 kV and 25 mA. The X-ray optics used was the standard Bragg-Brentano para-focusing mode with the X-ray diverging from a DS slit (1 mm) at the tube to strike the sample and then to converge at a position sensitive X-ray detector (Lynx-Eye, Bruker-AXS). The two-circle 218 mm diameter θ θ goniometer was computer controlled with independent stepper motors and optical encoders for the circle with the smallest angular step size of 0.0001. The software suite for data collection and evaluation is windows based. Data collection is an automated COMMANDER program employing a DQL file. The program EVA analyzed data. CuK α energy is 8.04 keV, which corresponds to an x-ray wavelength of 1.5406 Å. The anti-scatter slit was 12.530 mm, and the divergence slit was 1.00mm. The knife edge was used for anti-air-scatter, and the scan type completed was the coupled theta. The goniometer radius was 217.5 mm. The step size was 0.015, with a start of 5.0 and an end of 70.0.
- 2.4.3 Dynamic Light Scattering (DLS). Small aliquots of alginate-coated IONPs were taken and diluted with milli-Q water filtered with a 0.2-micron filter. The samples were placed in a cuvette and placed in the Malvern Panalytical Zetasizer Nano. The samples were measured three times to ensure accuracy.
- 2.4.4 Zeta Potential. Small aliquots of alginate-coated IONPs were taken and diluted with milli-Q water filtered with a 0.2-micron filter. The samples were then placed in a cuvette and placed in Zetasizer Nano ZS. The zeta potential of the samples was then measured three times to ensure correct measurements.

2.5 Human cell lines

Cells were purchased through ATCC and stored in liquid nitrogen. The cells were thawed, resuspended in media, and centrifuged. Once centrifuged, the culture media was removed. Fresh media was then added to the tube and mixed gently. The media and cells were plated in a sterile tissue culture flask. Human gingival fibroblasts (HGFB) were incubated in Dulbecco's Modified Eagle Medium (DMEM) with 10% Fetal bovine serum (FBS) and penicillin/streptomycin at 37.0 °C under 5% carbon dioxide and maintained until they were confluent. TIGK cells (human gingival keratinocytes) were grown in Keratinocyte Serum-free Medium (KSFM, ThermoFisher Cat no. 17005042) with the supplemental keratinocyte growth kit and penicillin/streptomycin at 37.0 °C under 5% carbon dioxide and maintained until they were confluent.

2.6 Bacterial growth

2.6.1 Streptococcus oralis, Streptococcus mitis, Streptococcus gordonii, Veionella parvula, and Fusobacterium nucleatum. All bacteria were purchased through ATCC; upon arrival, bacteria were plated on Tryptic soy medium with 5% defibrinated sheep blood. Tryptic soy agar and broth were mixed with deionized water and autoclaved. The agar and broth were cooled to around 47 °C, and defibrinated sleep blood was added. The agar was then set aside to harden. The bacteria were streaked onto plates and left to grow in anaerobic conditions until colonies were visible (1-3 days). Once colonies were formed, a single colony was removed and placed in a small tube containing broth and 50 % glycerol. Frozen stock

was stored at -80 °C. Once needed, the bacteria were removed from the -80°C storage and placed in an incubator at in sterile media at 37 °C. The bacteria were maintained in anaerobic conditions and liquid media was replaced every 2-3 days.

2.6.2 Porphyromonas gingivalis. P. gingivalis was purchased through ATCC; upon arrival, bacteria were plated on supplemented tryptic soy medium. The supplemented tryptic soy medium was made with tryptic soy broth, yeast extract, L-cysteine hydrochloride, hemin stock, vitamin K1 stock, and DI water. The mixture was then autoclaved at 121 °C prior to use. The bacteria were left to grow in anaerobic conditions for two days on the agar plates. Once colonies were formed, a single colony was removed and placed in a small tube containing broth and 50% glycerol. The samples were then stored at -80 °C. Once needed, the bacteria were removed from the -80 °C storage and placed in an incubator at 37 °C. The bacteria were grown in anaerobic conditions with the liquid media replaced every 2-3 days until placed for testing.

2.7 MTT assay

2.7.1 Human cells. Human cells were grown to confluency harvested and quantified using a hemocytometer. The cells were resuspended with fresh medium and plated at 10,000 cells per well in a 96-well plate. The well plate was then placed in the incubator to grow overnight. Once the cells adhered to the plate, the cells were treated with high (50 mg/mL), mid (5 mg/mL), and low (0.5 mg/mL) concentrations of IONPs. The cells were treated for 15 minutes, and a static magnetic field was applied for 2 mins (1 minute North and 1 minute south) to cause the particles to "scrub", the total contact time was ~40 minutes, including the rinse time. The media was removed, and the cells were rinsed with sterile Dulbecco's phosphate-buffered saline (DPBS). MTT (3-[4,5-dimethylthiazol-2-yl]-2,5 diphenyl tetrazolium bromide) assays were performed in 96-well plates. In each well, 50 microliters of MTT solution and 50 microliters of serum-free media were added. The cells were placed into the incubator for 3 hours. After 3 hours, 150 microliters of MTT solvent were added to each well. The plate was then wrapped in foil and placed on a shaker plate for 15 minutes. The absorbance was read at 590 nm with a BioTek Cytation 5.

2.7.2 Bacterial Cells. MTT assay of bacteria has been shown to be unreliable for accurate measurements due to the varying coloration of the media being used [14]. To avoid this issue, the bacteria were plated on a sterile 96-well plate and grown in optically clear artificial saliva. The bacteria were plated at $1x10^9$ cfu/well and anaerobically incubated for 24 hours prior to treatment. The excess media was removed from the wells and treated with various types and concentrations of IONPs.

We tested the effects of 0.05% (0.05 mg/mL), 0.5% (5 mg/mL), and 5% (50 mg/mL) concentrations of alginate-coated samples #1, #2, #3, and #4, and a 0.5% (5 mg/mL) concentration of dextran-coated samples #1 and #4. Once treated, a magnet was applied to the outside of the wells and manipulated to cause the particles to scrub. The magnetite was applied for 2 minutes total, and the total time of treatment was 30 minutes, including rinse times. Each well contained 50 microliters of MTT solution and 50 microliters of artificial saliva. The bacteria were incubated for 3 hours; afterward, 150 microliters of MTT solvent were added. The plate was then wrapped in foil and shocked for 15 minutes on a plate shaker. The absorbance was then read at 570 nm with a BioTek Cytation 5 plate reader.

0.4 µm Transwell Plate with Insert

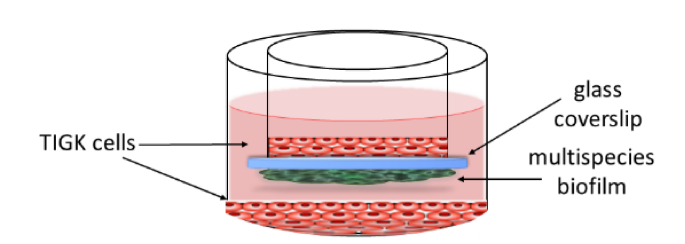


Figure 1. Schematic of TIGK cell co-culture with multispecies biofilm grown on glass coverslip and affixed to the inside of the insert in a transwell plate.

2.8 Establishment of a multispecies biofilm human TIGKs cell co-culture

An in vitro periodontal biofilm model was established after [15]. TIGK cells, a human immortalized keratinocyte cell line (ATCC), was grown to 80% confluence in KSFM, and then removed with 0.05% trypsin, washed in DPBS and seeded at approximately 1×10^5 cells per mL on the bottom of the plate an on the insert of a 12-well transwell plate having 12 mm inserts and a 0.4 µm membrane (VWR North America) as described previously [15, 16]. The cells were then challenged with inverted multispecies biofilms as follows: *S. mitis* was standardized at 1×10^7 cfu/mL plated onto sterile coverslips, and grown in anaerobic conditions at 37 °C for 24-hours, at which time 1×10^7 cfu/mL of *F. nucleatem* was added to the culture and the plates were returned to incubation under anaerobic conditions as before, 24-hours later 1×10^7 cfu/mL of *P*.

gingivalis was added to the culture and the multispecies biofilm was incubated anaerobically for four days. Two groups of multispecies biofilms were treated with either sample #3 or sample #4 low-dose (0.5 mg/mL) IONPs coated with alginate.

Table 1: Primers used for qPCR, with the forward and reverse genes.

Genes	Forward Primer (5'-3')	Reverse Primer (5'-3')
GAPDH	CAAGGCTGAGAACGGGAAG	GGTGGTGAAGACGCCAGT
il-1α	ATCATGTAAGCTATGGCCCACT	CTTCCCGTTGGTTGCTACTAC
il-1β	CTCGCCAGTGAAATGATGGCT	GTCGGAGATTCGTAGCTGGAT
il-6	AAATTCGGTACATCCTCGACGG	GGAAGGTTCAGGTTGTTTTCTGC
il-8	TTTTGCCAAGGAGTGCTAAAGA	AACCCTCTGCACCCAGTTTTC

The biofilms were treated for 25 minutes with the magnetic field applied for 1 minute facing North and one minute facing South with a back-and-forth motion applied. The total exposure time was 40 minutes including the time required to perform four post-treatment washes with DPBS. The treated and untreated bacterial

biofilms on coverslips were then attached to the inserts on the transwell using sterile Vaseline with the biofilm facing down. One group was kept as a control and was not challenged with the multispecies biofilm. The biofilms were grown together with the TIGKs in antibiotic-free KSFM for 24 hours at 37 °C and 5% CO₂. After that, cellular RNA was harvested using TRIZOL and qPCR of selected inflammatory cytokines was completed using GADPH used as the housekeeping reference gene (Table 1).

2.9 Statistical Analysis

Graphical and statistical analyses were performed on Prism GraphPad. Statistical analysis of MTT data was performed using Brown-Forsythe and Welch ANOVA. Statistical analysis of qPCR data was entered into Prism, and one outlier was identified and removed from the data set. D'Agostino-Pearson, Shapiro-Wilk, and Kolmogorov-Smirnov tests were performed to check for normal Gaussian distributions, our data failed two out of three normality tests, so we used Mann-Whitney test and multivariable ANOVA to determine the statistical significance of replicates vs. control

3. RESULTS

3.1 Characterization of IONPs

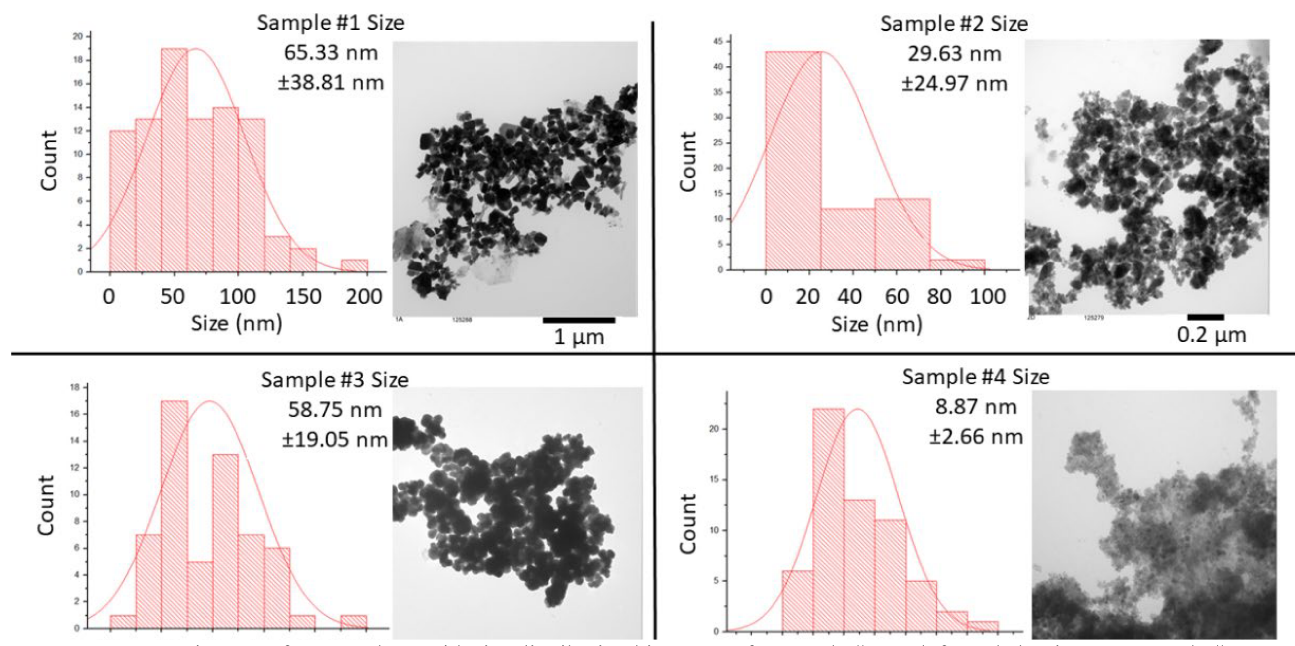


Figure 2. TEM images of IONPs along with size distribution histograms for sample #1 top left, scale bar is 1 μ m; sample #2 top right, scale bar is 0.2 μ m; sample #3 bottom left, scale bar is 2 μ m; and sample #4 bottom right, scale bar is 200 nm.

3.1.1 TEM Images. TEM images were taken of all four variations of the IONPs, and sizes were measured using ImageJ and plotted in Origin. Sample #1 had a relatively broad size distribution with a mean size of 65.33 nm \pm 38.81 nm, sample #2 had a mean size of 29.62 nm \pm 24.97 nm, sample #3 had a mean size of 58.75 nm \pm 19.05 nm, and sample #4 had a mean size of 8.87 nm \pm 2.66 nm (Figure 2).

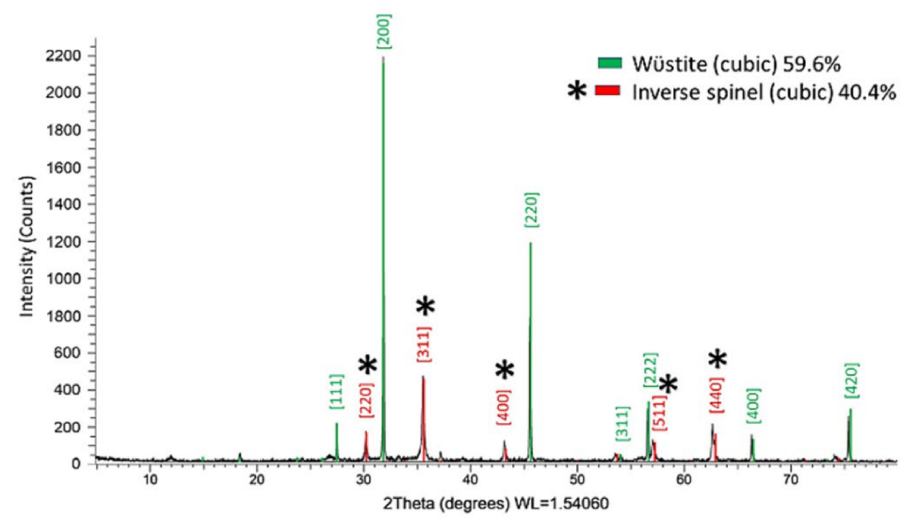


Figure 3. XRD spectrum of the synthesized IONPs (sample #1) prior to the polymer coating.

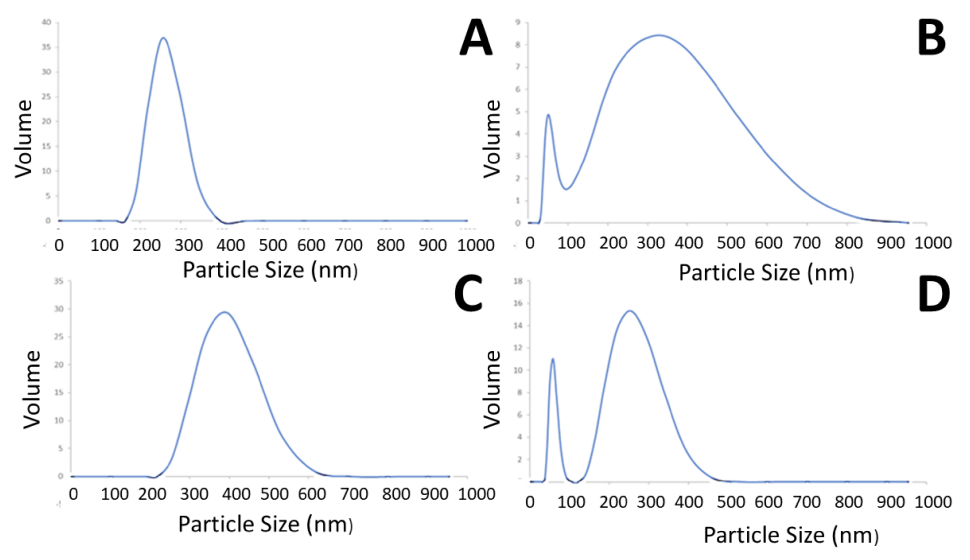


Figure 4. DLS spectra of all IONPs samples coated with alginate. A-D represents samples #1 to #4, respectively.

3.1.2 XRD results. XRD analysis performed sample #1 prior to coating with alginate or dextran reveals that the crystalline structure of the IONPs consists of multi-phase iron oxide with $\sim 40\%$ corresponding to the cubic spinel phase which may be attributed to either Fe₃O₄ or Fe₂O₃, these phases are difficult to distinguish between using XRD, the ~60% remaining corresponds the to nonstoichiometric Wüstite phase of iron oxide, which has face-centered cubic (FCC) packing (Figure 3).

3.1.3 Dynamic scattering. DLS analyses revealed the hydrodynamic size of the alginate coated IONPs. In Figure 4. B and D two peaks are apparent, due to agglomeration. The volume totals are shown. According to the DLS spectra, sample #1 (Figure 4 A) has a hydrodynamic particle size of ~250 nm, sample #2 (Figure 4 B) has a hydrodynamic particle size of ~50 nm, sample #3 (Figure 4 C) has a hydrodynamic particle size of \sim 400 nm, and sample #4 (Figure 4 D) has

hydrodynamic particle size of ~50 nm. Agglomeration and flocculation can lead to various results and size ranges and is a function of the density, solvent, nanoparticle coatings, surfactants, and temperature. Addressing the colloidal stability issue is a critical parameter in developing an efficacious nanoparticle system that exhibits the desired behaviors as a dynamic system. This is especially important considering the salinity and protein concentrations in a biological environment.

3.1.4 Zeta Potential Measurements. Zeta potential results revealed that all four of the IONP samples all exhibit a negative zeta potential value and are colloidally stable in pure water when coated with alginate (Figure 5). Sample #1 had a zeta potential of -42.5 mV, sample #2 had a value of -29.4 mV, sample #3 had a value of -33.5mV, and sample #4 had a value of -41.6 mV.

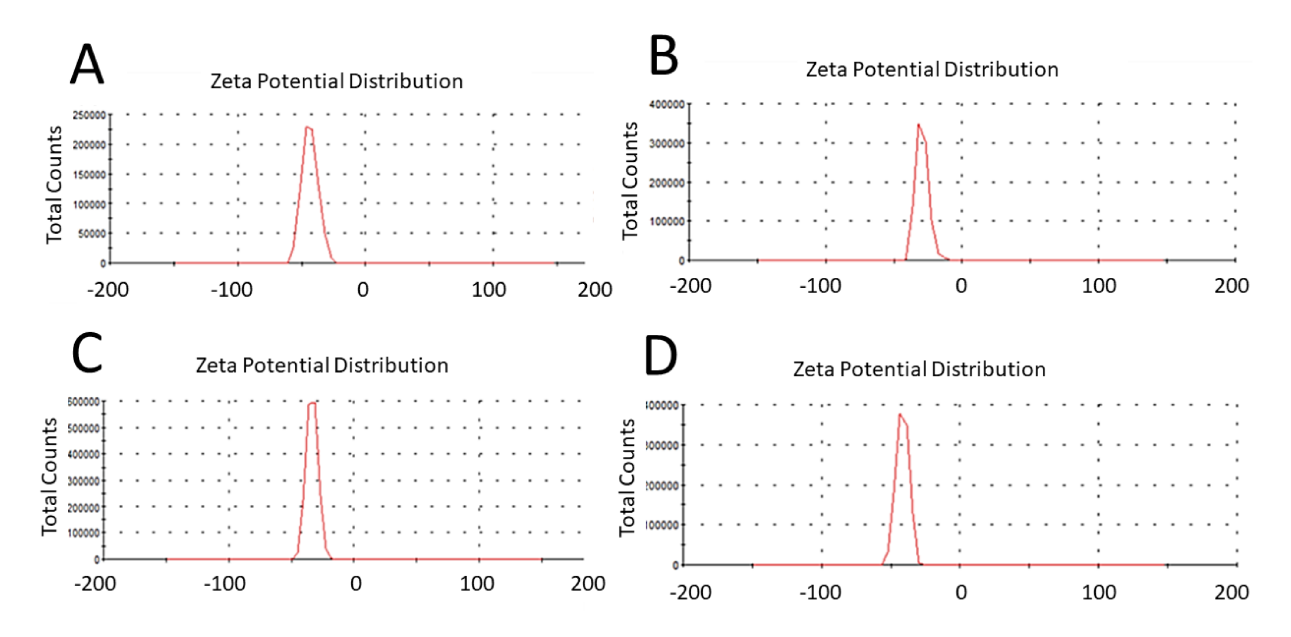


Figure 5. Zeta potential results for the alginate coated IONPs used in the experiments. A corresponds to sample #1, B corresponds to sample #2, C corresponds to sample #3, and D corresponds to sample #4.

3.2 MTT Assays

3.2.1 Human gingival fibroblast viability. The viability of gingival fibroblast cells was completed with the alginate coated sample #1 IONPs synthesized in our laboratory. Figure 6 reveals the results of low (0.05%), mid (0.5%), and high (5%) doses of sample #1 IONPs diluted with sterile DPBS. We did not observe any statistically significant reduction in viability compared to the control group. Alginate-coated IONPs were found to have no change in the cell's physical and physiological health per this metabolic assay.

3.2.2 Porphyromonas gingivalis viability. The MTT results of P. gingivalis that were treated with all IONPs samples and both coatings are shown in Figure 7. A statistically significant reduction in viability was observed for alginate-coated sample #3 (A3) at the low and mid concentrations with a pvalue of 0.0455 and 0.0349, respectively and alginate coated sample #4 (A4) at low, mid, and concentrations returned p-values of 0.0138 and 0.0045, 0.0230, respectively. Only sample #1 of the dextran-coated particles exhibited a statistically significant reduction in viability at the 0.05 mg/mL (low) concentration with a p-value of 0.0219 (Figure 6). Low and mid dose alginate coated sample #4 was found to be the most effective against P. gingivalis. Possibly due to agglomeration at the higher concentrations, which may reduce distribution through the biofilm pores.

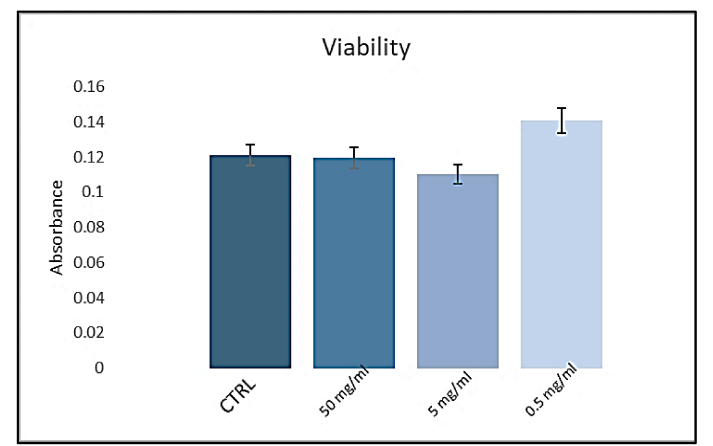


Figure 6. Viability of human gingival fibroblast cells treated with various concentrations of alginate coated IONPs (sample #1). No toxicity was found at any concentration points tested. The error bars show the standard deviation of the results.

3.2.3 Co-culture, qPCR of TIGK Cells The in vitro

periodontal biofilm model in which gingival keratinocyte cultures were challenged with multispecies biofilms and treated with IONPs revealed a trend of increased inflammation in the untreated biofilm co-culture exactly what is observed in periodontal disease. We observe a reduction in inflammation in the cells treated with alginate coated sample #3 and no

P. gingivalis Viability

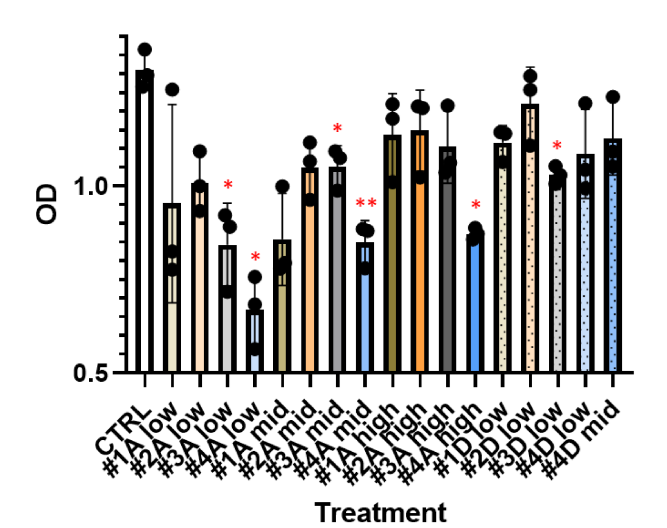


Figure 7: MTT assay of *P.gingivitis* treated with all IONPs synthesized and coated with alginate and dextran. As seen in the figure, "A" represents IONPs that are coated with alginate, and "D" represents IONPs coated with dextran. The numbers correspond to samples #1-4. The treatment concentrations were 0.05 mg/mL (low), 0.5 mg/mL (mid), and 50 mg/mL (high). A single red asterisk denotes statistical significance, a double asterisk represents high statistical significance. The error bars represent the standard deviation.

inflammation above control was observed in the biofilmchallenged group treated with sample #4 (ultrasmall IONPs coated with alginate (Figure 8). Although these values did not reach statistical significance, likely due to the small sample size (n=4) and the large range of standard deviations in the untreated biofilm group, we did observe a clear trend of increased inflammatory gene expression in the biofilm challenged TIGK cells (Figure. 8). That inflammation was reduced in the biofilm-challenged cells treated with alginate coated sample #3 and completely absent in the biofilm-challenged cells treated with the ultrasmall alginate-coated iron oxide (sample #4). This finding supports the findings of the MTT assay, and it appears that sample #4, and possibly smaller particles in general are most effective against multispecies biofilms as well and do not appear to induce inflammation in the gingival keratinocytes.

4. DISCUSSION

Characterization of the IONPs was performed to gather an in-depth understanding of the materials before being used on trials. The XRD showed that the particles tested were a mixture of mainly magnetite phase with a small amount in the Wüstite phase. The ideal particle would have a high composition of γ -Fe₂O₃ or Fe₃O₄ because these phases have ferromagnetic ordering. This is the first time IONPs of different sizes, and different phases of iron oxide have

had their antimicrobial properties directly compared. It appears that black iron oxide (sample #3) had better antimicrobial properties than red iron oxide (sample #2) although size-effects may also play a role in this finding. In general, IONPs appear to be non-toxic to mammalian cells at the concentrations investigated. However, their antimicrobial properties are not so simple, but rather appear strongly dependent on the phase, size, and functionalization.

The functionalization and size also appeared to significantly influence antimicrobial efficacy of the particles. It appears from these findings that smaller-sized IONPs are more effective antimicrobials, and alginate may enhance this property. We observed significantly enhanced results against P. gingivalis bacteria when they were treated with alginate coated IONPs as opposed to dextran coated. Additionally, it was apparent that the smaller IONPs were also more effective at all concentrations. We did observe an enhanced antimicrobial effect in the

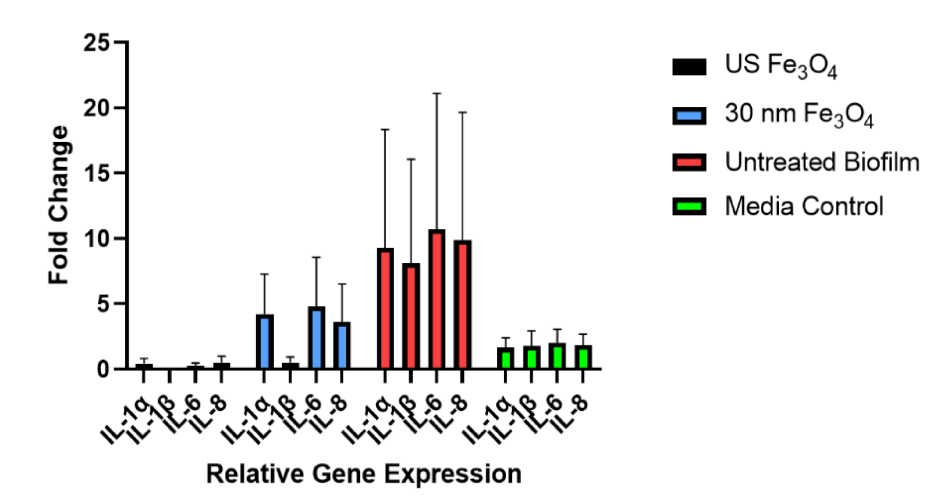


Figure 8. Gene relative gene expression of four inflammatory markers taken from TIGK cells treated with media alone (green), untreated multispecies biofilm (red), and biofilm treated with alginate coated IONPs sample #3 (blue) or sample #4 (black). The error bars shown represent the standard error of the mean values.

higher treatment concentration groups in this study, likely due to agglomeration that results in larger hydrodynamic particle sizes in the higher concentration groups. We also observed this trend in DLS measurements. In this study, treatments were all applied in liquid medium or artificial saliva, but it may be possible to engineer a gel or solution with better colloidal stability in the biological fluids such that particles are maintained as single particles, rather than agglomerates, to investigate higher concentrations.

In addition, we were able to verify the safety and efficacy of IONP anti-biofilm activities with a human keratinocyte/multispecies biofilm model that closely simulates periodontal disease in humans. Although our results did not reach statistical significance, we were able to verify the superior action of the ultrasmall, alginate coated IONPs (sample #4) compared to the larger magnetite IONPs. This finding will allow us to optimize this system for our application. The antimicrobial effects appear to be sufficient at the low dose, well below dosages of iron which could cause toxicity in humans. These results suggest that IONP treatment could eradicate pathogenic bacteria and end the chronic inflammatory state characteristic of periodontal diseases.

Acknowledgments

The authors thank Nin Gan and Chi Huang at the TAMU-CC Laboratory for Environmental Health for their support and Texas A&M University-Corpus Christi undergraduate students Nicole Murphy, Brooke McCormick, Corbin Garcie, Margie Alvarez, Xitlali Gallegos-Cruz, and Julia Stinson for general laboratory assistance. This work was supported in part by NSF STTR 2151653.

Notes

Leisha Armijo declares corporate affiliations with MNT SmartSolutions and LEI nanoTech.

REFERENCES

- [1] Wang, D., Haapasalo, M., Gao, Y., Ma, J. and Shen. Y., "Antibiofilm peptides against biofilms on titanium and hydroxyapatite surfaces," Bioactive Materials 3(4), 418-425 (2018).
- [2] Flemming, H., Neu, T. R., and Wozniak. D. J., "The EPS matrix: the "house of biofilm cells"," Journal of Bacteriology 189(22), 7945-7947 (2007).
- [3] Mann, E. E., Rice, K. C., Boles, B. R., Endres, J. L., Ranjit, D., Chandramohan, L., Tsang, L. H., Smeltzer, M. S., Horswill, A. R. and Bayles, K. W., "Modulation of eDNA release and degradation affects *Staphylococcus aureus* biofilm maturation," PloS one, 4(6), e5822 (2009).
- [4] Armijo, L. M., Wawrzyniec, S. J., Kopciuch, M., Brandt, Y. I, Rivera, A. C., Withers, N. J., Cook, N. C., Huber, D. L., Monson, T. C., Smyth, H. D. C. and Osiński, M., "Antibacterial activity of iron oxide, iron nitride, and tobramycin conjugated nanoparticles against *Pseudomonas aeruginosa* biofilms," Journal of Nanobiotechnology 18(1), 1-27 (2020).
- [5] Thurnheer, T., and Belibasakis, G.N., "Streptococcus oralis maintains homeostasis in oral biofilms by antagonizing the cariogenic pathogen Streptococcus mutans," Molecular Oral Microbiology 33(3), 234-239 (2018).
- [6] "Health and Economic Benefits of Oral Diseases Interventions." Centers for Disease Control and Prevention, Centers for Disease Control and Prevention, https://www.cdc.gov/chronicdisease/programs-impact/pop/oral-disease.htm (2022).
- [7] "Oral Health." World Health Organization, World Health Organization, https://www.who.int/news-room/fact-sheets/detail/oral-health (2022).
- [8] Brookes, L. S., Bescos, R., Belfield, L. A., Ali, K., and Roberts, A., "Current uses of chlorhexidine for management of oral disease: a narrative review," Journal of Dentistry 103, 103497 (2020).
- [9] Bandara, H. M., Nguyen, D., Mogarala, S., Osiñski, M., Smyth, H. D., "Magnetic fields suppress *Pseudomonas aeruginosa* biofilms and enhance ciprofloxacin activity," Biofouling 31(5), 443-57 (2015).

- [10] Alas, G., Pagano, R.E., Nguyen, J.Q., Bandara, H.N., Ivanov, S.A., Smolyakov, G.A., Huber, D.L., Smyth, H.D., Osiński, M., "Effects of iron-oxide nanoparticles and magnetic fields on oral biofilms," Colloidal Nanoparticles for Biomedical Applications XII. SPIE. 10078, 9-20 (2017)
- [11] Park, J., An, K., Hwang, Y., Park, J. G., Noh, H. J., Kim, J. Y., Park, J. H., Hwang, N. M. and Hyeon, T., "Ultralarge-scale syntheses of monodisperse nanocrystals," Nature Materials 3(12), 891-895 (2004).
- [12] Martin, L.M., Sheng, J., Zimba, P.V., Zhu, L., Fadare, O.O., Haley, C., Wang, M., Phillips, T. D., Conkle, J., and Xu, W., "Testing an iron oxide nanoparticle-based method for magnetic separation of nanoplastics and microplastics from water," Nanomaterials 12(14), 2348 (2022).
- [13] Sun, S., and Zeng, H., "Size-controlled synthesis of magnetite nanoparticles," Journal of the American Chemical Society, 124(28), 8204-8205 (2002).
- [14] Benov, L., "Effect of growth media on the MTT colorimetric assay in bacteria," PLOS One, 14(8), e0219713 (2019).
- [15] Millhouse, E., Jose, A., Sherry, L., Lappin, D. F., Patel, N., Middleton, A. M., Pratten, J., Culshaw, S. and Ramage, G., "Development of an *in vitro* periodontal biofilm model for assessing antimicrobial and host modulatory effects of bioactive molecules," BMC Oral Health 14(80), (2014).
- [16] Bates, A. M., Fischer, C. L., Abhyankar, V. P., Johnson, G. K., Guthmiller, J. M., Progulske-Fox, A. and Brogden, K. A., "Matrix metalloproteinase response of dendritic cell, gingival epithelial keratinocyte, and T-cell transwell co-cultures treated with *Porphyromonas gingivalis* hemagglutinin-B," International Journal of Molecular Sciences 19(12), 3923 (2018).